



**MOLECULAR SIMULATION STUDY OF CONDENSATION AND  
EVAPORATION OF MIXTURES CO<sub>2</sub>, CH<sub>4</sub> AND H<sub>2</sub>O IN THE  
SLIT-PORE**



**Natnaree Soitaku  
Sutasinee Sooksai**

**A Thesis Submitted in Partial Fulfillment of the Requirements for the  
Bachelor Degree in Chemical Engineering  
Naresuan University  
Academic Year 2014**



การศึกษาแบบจำลองเชิงโมเลกุลของการควบแน่นและการระเหยของสารผสม  
ระหว่างแก๊สคาร์บอนไดออกไซด์ มีเทน และน้ำ ในรูปพหุคูณแบบสลิท



นางสาวณัชนรี สร้อยตะคุ รหัส 54362814

นางสาวสุธาสินี สุกใส รหัส 54362999

ห้องปฏิบัติการวิศวกรรมศาสตร์
วันที่รับ..... 30 ต.ค. 2558
เลขทะเบียน..... 16902881
เลขที่เอกสาร..... ๒๓
มหาวิทยาลัยเกษตรศาสตร์ ๒๖ ๑ ๑

2558

ปริญญานิพนธ์นี้เป็นส่วนหนึ่งของการศึกษาหลักสูตรปริญญาวิศวกรรมศาสตรบัณฑิต

สาขาวิชาวิศวกรรมเคมี ภาควิชาวิศวกรรมอุตสาหกรรม

คณะวิศวกรรมศาสตร์ มหาวิทยาลัยเกษตร

ปีการศึกษา 2557



## ใบรับรองปริญญาโท

ชื่อหัวข้อโครงการ การศึกษาแบบจำลองเชิงโมเดลของการควมแน่นและการระเหยของสาร  
ผสมระหว่างแก๊สคาร์บอนไดออกไซด์ มีเทน และน้ำ ในรูปพุนแบบสลิท

ผู้ดำเนินโครงการ นางสาวณัชชรี สร้อยตะคุ รหัส 54362814  
นางสาวสุธาสินี สุกใส รหัส 54362999

ที่ปรึกษาโครงการ ดร.นิคม กลมเกลี้ยง

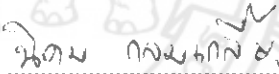
ที่ปรึกษาร่วมโครงการ อาจารย์อภาภรณ์ จันทร์ปรีกษ์

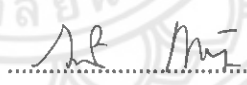
สาขาวิชา วิศวกรรมเคมี

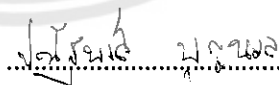
ภาควิชา วิศวกรรมอุตสาหกรรม

ปีการศึกษา 2557

คณะวิศวกรรมศาสตร์ มหาวิทยาลัยนเรศวร อนุมัติให้ปริญญาโทฉบับนี้เป็นส่วนหนึ่งของการศึกษาตามหลักสูตรวิศวกรรมศาสตรบัณฑิต สาขาวิชาวิศวกรรมเคมี

  
.....ที่ปรึกษาโครงการ  
(ดร.นิคม กลมเกลี้ยง)

  
.....กรรมการ  
(รองศาสตราจารย์ ดร.สมร หิรัญประดิษฐ์กุล)

  
.....กรรมการ  
(ดร.ปณัฐพงศ์ บุญวง)

  
.....กรรมการ  
(อาจารย์อภาภรณ์ จันทร์ปรีกษ์)

ชื่อหัวข้อโครงการ	การศึกษาแบบจำลองเชิงโมเลกุลของการควบแน่นและการระเหยของสารผสมระหว่างแก๊สคาร์บอนไดออกไซด์ มีเทน และน้ำ ในรูปพหุแบบสลิท		
ผู้ดำเนินโครงการ	นางสาวณัชนรี	สร้อยตะคุ	รหัส 54362814
	นางสาวสุธาสินี	สุกใส	รหัส 54362999
ที่ปรึกษาโครงการ	ดร.นิคม	กลมเกลี้ยง	
ที่ปรึกษาร่วมโครงการ	อาจารย์อาภาภรณ์	จันทร์ปรัักษ์	
สาขาวิชา	วิศวกรรมเคมี		
ภาควิชา	วิศวกรรมอุตสาหกรรม		
ปีการศึกษา	2557		

### บทคัดย่อ

การศึกษากการประมวลผลเชิงโมเลกุลของการควบแน่นและการระเหยของสารผสมระหว่างแก๊สคาร์บอนไดออกไซด์ มีเทน และน้ำ ในรูปพหุแบบสลิท โดยใช้แบบจำลองแกรนด์ คาร์โนนิคอลลมอลติคาร์โล (Grand Canonical Monte Carlo, GCMC) พบว่าไม่มีวงรอบฮีสเทอโรสิสของแก๊สคาร์บอนไดออกไซด์ และมีเทน ที่อุณหภูมิสูงกว่าอุณหภูมิวิกฤตของฮีสเทอโรสิส เนื่องจากที่อุณหภูมิสูง สมรรถนะการแยกระหว่างแก๊สคาร์บอนไดออกไซด์ และมีเทน ลดลงเมื่ออุณหภูมิสูงขึ้น ซึ่งในส่วนนี้สามารถนำไปประยุกต์ใช้ ในการแยกแก๊สออกจากถ่านหินได้ เป็นที่น่าสนใจว่า ปริมาณการถูกดูดซับของคาร์บอนไดออกไซด์ จากสารผสมระหว่างแก๊สคาร์บอนไดออกไซด์ และมีเทนมีค่าเพิ่มขึ้น เมื่ออุณหภูมิลดลง ซึ่งสอดคล้องกับสิ่งที่พบได้กับการดูดซับแก๊สบริสุทธิ์ แต่กลับได้ผลตรงกันข้ามสำหรับการดูดซับมีเทนในสารผสมระหว่างแก๊สคาร์บอนไดออกไซด์ และมีเทน มากไปกว่านั้น วงรอบฮีสเทอโรสิสของแก๊สคาร์บอนไดออกไซด์ และมีเทนในรูปพหุแบบสลิท ที่อุณหภูมิ 300 เคลวิน ไม่สามารถเกิดขึ้นได้ แต่ในทางตรงกันข้ามเมื่อน้ำเข้ามาเจือปนในสารผสม วงรอบฮีสเทอโรสิสของแก๊สคาร์บอนไดออกไซด์ และมีเทนในรูปพหุชนิดเดียวกัน และอุณหภูมิเดียวกันสามารถเกิดขึ้นได้เนื่องจากการเรียงตัวกันของน้ำในระหว่างการควบแน่นของน้ำไปลดพื้นที่ในการดูดซับ ซึ่งเล็กเพียงพอที่จะทำให้แก๊สคาร์บอนไดออกไซด์ และมีเทนสามารถควบแน่นได้

**Title** Molecular simulation study of condensation and evaporation of CO<sub>2</sub>, CH<sub>4</sub> and H<sub>2</sub>O mixtures in a slit-pore

**Author** Miss Natnaree Soitaku  
Miss Sutasinee Sooksai

**Advisor** Dr.Nikom Klomkliang Ph.D.

**Co-Advisor** Miss Arphaphon Chanpirak

**Academic Paper** Thesis B.ENG. in Chemical Engineering,  
Naresuan University, 2014

**Keyword** Hysteresis loop; Mixture; Adsorption; Slit-pore;  
Condensation; Evaporation

---


### Abstract

We study condensation and evaporation of CO<sub>2</sub> and CH<sub>4</sub> mixtures in the presence of water in a graphite slit-mesopore by using grand canonical Monte Carlo simulation. The hysteresis loop of CO<sub>2</sub> and CH<sub>4</sub> is disappeared at temperature higher than the critical hysteresis value due to the high thermal motion. The selectivity between CO<sub>2</sub> and CH<sub>4</sub> is decreased with temperature increase which is able to apply for coal seam gas separation. Interestingly, in the CO<sub>2</sub>/CH<sub>4</sub> mixture adsorption, the uptake of the dominant CO<sub>2</sub> is increased when temperature is decreased which is similar to that of pure component adsorption but it is opposite for the weaker CH<sub>4</sub>. In addition, the hysteresis loop of CO<sub>2</sub>/CH<sub>4</sub> mixture adsorption in slit-pore at 300 K cannot be found. In contrast, when water is presented in the mixtures the hysteresis loop of CO<sub>2</sub> and CH<sub>4</sub> in the pore at 300K is observed. Because water clusters (during the condensation process) reduce the adsorbed space (where CO<sub>2</sub> and CH<sub>4</sub> can condense) under that state.

## ACKNOWLEDGEMENTS

We would like to express our appreciation to our thesis examining committee for their inventive questions and guidance. We are most grateful to our thesis Dr.Nikom Klomkliang who is advisor and supporter information. He encourage that have helped us pass through our difficult times And Miss Arphaphon Chanpirak who is co-advisor for the best advice.

We would like to thank all of the lecturers at the School of Chemical Engineering, Naresuan University (NU) for their good attitude and advice. We would also like to thank all of our friends who are graduate students in the School of Chemical Engineering, who shared the experience and knowledge. We would like to express our honest gratefulness to everyone in our family, especially our parents for their love and care. We would like to thank the Thailand Research Fund (Contract no.TRG5780126) for support this project. Finally, we gratefully acknowledge the invaluable help of everyone we may have forgotten to mention here.



Natnaree Soitaku  
Sutasinee Sooksai  
May 2015

# LIST OF CONTENTS

	<b>Page</b>
ABSTRACT (THAI).....	I
ABSTRACT (ENGLISH).....	II
ACKNOWLEDGEMENTS.....	III
LIST OF CONTENTS.....	IV
LIST OF TABLES.....	VI
LIST OF FIGURES.....	VII
<b>CHAPTER</b>	
<b>I INTRODUCTION AND LITERATURE REVIEW .....</b>	<b>1</b>
1.1 Significance of the problem.....	1
1.2 Literature review.....	1
1.3 Research Objectives.....	2
1.4 Outcomes.....	2
1.5 Scope.....	3
<b>II THEORY AND METHODOLOGY.....</b>	<b>4</b>
2.1 Gas adsorption.....	4
2.2 Variables affecting the adsorption isotherm.....	5
2.3 Intermolecular potentials.....	6
2.4 Methodology.....	10
<b>III RESULTS AND DISCUSSIONS.....</b>	<b>13</b>
3.1 Adsorption of CO <sub>2</sub> /CH <sub>4</sub> mixture.....	13
3.2 Adsorption of CO <sub>2</sub> /H <sub>2</sub> O and CH <sub>4</sub> /H <sub>2</sub> O mixtures.....	16
3.3 Adsorption of CO <sub>2</sub> /CH <sub>4</sub> /H <sub>2</sub> O mixture.....	19
<b>IV CONCLUSIONS.....</b>	<b>22</b>

**LIST OF CONTENTS (CONT.)**

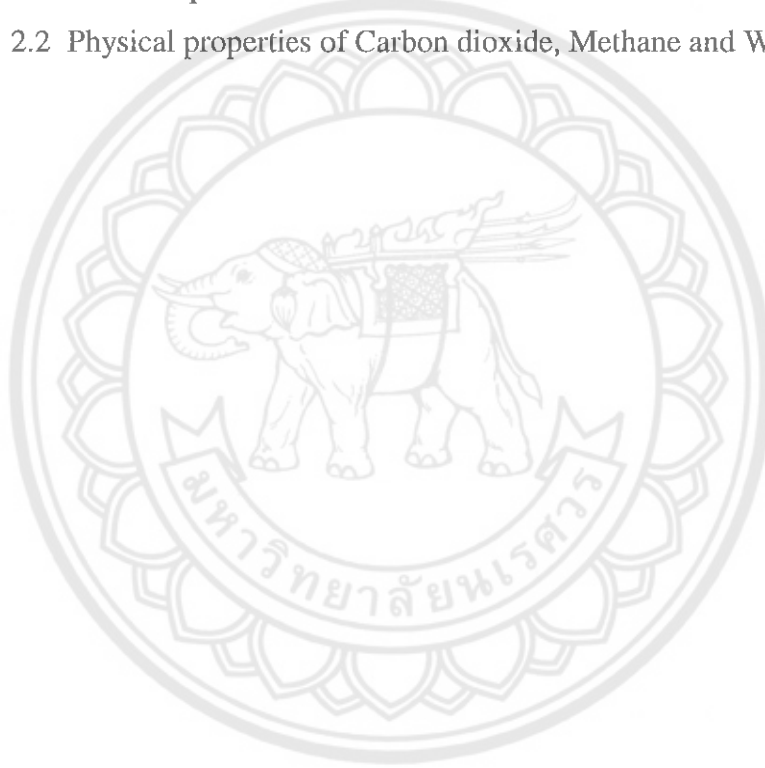
	<b>Page</b>
<b>REFERENCES</b> .....	23
<b>APPENDIX</b> .....	30
<b>BIOGRAPHY</b> .....	35





## LIST OF TABLES

Table	Page
1.1 First part, studying the case which has the same concentrations at 180 K, 220 K and 300 K.....	3
1.2 Second part, studying the case which has the same concentrations at 300 K.....	3
2.1 Potential parameters.....	6
2.2 Physical properties of Carbon dioxide, Methane and Water.....	8



## LIST OF FIGURES

Figure	Page
2.1 The IUPAC classification of hysteresis loop.....	5
2.2 The Models of fluid; (a) Model Methane. (b) Model Carbon dioxide and (c) Model Water TIP4P/2005.....	7
2.3 Graphitic slit-pore model.....	9
2.4 The grand canonical Monte Carlo (GCMC) simulation box.....	12
3.1 Adsorption-desorption of CO <sub>2</sub> /CH <sub>4</sub> mixture (1:1) in 3 nm width slit-pore at different temperature from 180-300 K; (a) CO <sub>2</sub> and CH <sub>4</sub> isotherm and (b) CH <sub>4</sub> isotherm.....	14
3.2 Snapshots of CO <sub>2</sub> /CH <sub>4</sub> mixture (1:1) adsorption in the slit-pore at (a) 180K and (b) 300 K, when monolayer is approximately completed.....	15
3.3 Adsorption-desorption of CO <sub>2</sub> /H <sub>2</sub> O mixture (1:1) in 3 nm width slit-pore at 300 K; (a) CO <sub>2</sub> and H <sub>2</sub> O isotherm and (b) CO <sub>2</sub> isotherm.....	17
3.4 Adsorption-desorption of CH <sub>4</sub> /H <sub>2</sub> O mixture (1:1) in 3 nm width slit-pore at 300 K; (a) CH <sub>4</sub> and H <sub>2</sub> O isotherm and (b) CH <sub>4</sub> isotherm.....	18
3.5 Adsorption-desorption of CO <sub>2</sub> /CH <sub>4</sub> /H <sub>2</sub> O mixture (1:1:1) in 3 nm width slit-pore at 300 K; (a) CO <sub>2</sub> , CH <sub>4</sub> and H <sub>2</sub> O isotherm, (b) CO <sub>2</sub> isotherm and (c) CH <sub>4</sub> isotherm.....	19
3.6 Snapshots of CO <sub>2</sub> /CH <sub>4</sub> /H <sub>2</sub> O mixture (1:1:1) in 3 nm width slit-pore at 300 K; (a) Adsorption at 40,000Pa and (b) Adsorption at 70,000Pa.....	21

# CHAPTER I

## INTRODUCTION AND LITERATURE REVIEW

### 1.1 Significance of the problem

In chemical industry, the design of industrial separation equipment and heterogeneous chemical reactors [1, 2] requires reliable methods for adsorption characterization of solids [3] and predicting single and mixture adsorption equilibria. In many cases the mixture equilibria is desired rather than pure. Therefore there are considerable interests to develop methods for predicting the adsorption equilibria of gas mixtures. Although mixture adsorption can be assessed experimentally, performing experiments that systematically explore the full range of potential operating conditions for a material of interest is time consuming. Because of that significant amount of work has been done on methods to predict mixture adsorption equilibria such as the lattice solution model by Lee [4], the two-dimensional gas model by Ross and Olivier [5], and the ideal adsorbed solution theory (IAST) by Myers and Prausnitz [6]. In recent years, with the improvement of high speed computer, it has been possible to solve the statistical mechanics problems of adsorption by using molecular simulation such as Monte Carlo (MC), Molecular Dynamics (MD) [7, 8] and Density Functional Theory [9, 10]. Molecular simulations can play a useful role in understanding mixture adsorption because in simulation to get an adsorption isotherm of gas mixtures is more straightforward and less time consuming than in experimental work. The use of molecular simulations has been extended to various works for example in understanding selectivity behaviour in mixture adsorption [11, 12] and, in separation studies of gas mixtures on metal-organic frameworks (MOF) [13-15].

### 1.2 Literature review

In the application of molecular simulations to the understanding and the prediction of adsorption properties of gas mixtures requires the development and the parameterization of potential models. Most of the studies on adsorption in the

literature utilize the use of the Lennard-Jones potential model (LJ) to describe the dispersive interaction between fluids. The use of LJ model is preferred especially for carbon because it is consistent with the usage of the well-known Steele model for solid-fluid interaction [16] and its molecular parameters are more readily available in the literature. Furthermore, the MC works well in the adsorption-desorption of simple gases such as argon, nitrogen, carbon dioxide, methane, and water at least for pure component adsorptions in ordered mesoporous solid [17-23]. The advantage of this study is the roles of fundamentals of adsorption that can be applied for solid characterization and gas separation.

Therefore, the main aim of this study is to study microscopically the capillary condensation and evaporation equilibrium of gas mixtures in a graphite slit-pore by using grand canonical Monte Carlo (GCMC) simulation. Because of the interest in natural gas separation [24-29], we will only focus on the adsorption of CO<sub>2</sub> and CH<sub>4</sub> mixtures. The work will first evaluate the methodology on mixture adsorption of CO<sub>2</sub> and CH<sub>4</sub> and then applied to mixture adsorptions of CO<sub>2</sub> and CH<sub>4</sub> in the presence of water.

### 1.3 Research objectives

1. To study mixture adsorption of CO<sub>2</sub> and CH<sub>4</sub> in slit-pore at 180 K, 220 K and 300 K.
2. To study mixture adsorption of CH<sub>4</sub>/H<sub>2</sub>O and CO<sub>2</sub>/H<sub>2</sub>O in slit-pore at 300 K.
3. To study mixture adsorption of CO<sub>2</sub>, CH<sub>4</sub> and H<sub>2</sub>O in slit-pore at 300 K.

### 1.4 Outcomes

The fundamental adsorption of the coal seam gas CH<sub>4</sub>/CO<sub>2</sub> with the presence of water will be seen in the level of macro and microscopic picture. Thus, the knowledge can be used to help the applications. This methods using GCMC simulation program performing in computer is the safe way. In addition, if it work, it will be a guideline for makes methane be efficiently and get the amounts which worth with costs.

### 1.5 Scope

This research work is divided into two main parts. The first part is focused on the equal compositions as listed in Table 1.1, and Table 1.2, respectively. The compositions in Table 1.2 are associated with the real conditions.

**Table 1.1 First parts, studying the case which has the same concentrations at 180 K, 220 K and 300 K.**

Methane	CO <sub>2</sub>	H <sub>2</sub> O
50%	50%	-

**Table 1.2 Second parts, studying the case which has the same concentrations at 300 K.**

Methane	CO <sub>2</sub>	H <sub>2</sub> O
50%	-	50%
-	50%	50%
33.3%	33.3%	33.3%
65%	20%	15%
65%	35%	-

## CHAPTER II

### THEORY AND METHODOLOGY

#### 2.1 Gas adsorption

Adsorption is a process that fluids (Adsorbate) interact with surface of solid (Adsorbent) on the surface or inside the pore. One of the key when the adsorption is deal with is the adsorption isotherm. The adsorption isotherm is obtained by measuring the uptake (The adsorbed amount) as a function of pressure at a given temperature. Adsorption isotherm can be demonstrated with the increase of pressure from the emptied pore (Adsorption) or with the decrease of pressure from the filled pore (Desorption). The hysteresis loop between the adsorption and desorption on adsorption on surface and in micropore (<2 nm) is mostly reversible. On the other hand, the hysteresis loop is definitely occurred in mesopore (2-50 nm) due to the cohesive adsorption [30-35].

The classification of hysteresis loop by IUPAC is shown in Figure 2.1 The adsorption and desorption branches of H1 are almost vertical and nearly parallel over an appreciable range of gas uptake. The adsorption and desorption branches of H4 are almost horizontal and nearly parallel over a wide range of relative pressure. The shapes of hysteresis loops are associated with specific pore structures. For example, porous materials which consist of well aligned, spheres and briquettes can produce an H1 type loop line, and materials of this type tend to have relatively narrow distributions of pore size. For the H2 type loops, the hysteresis loop is wide, and the desorption curve is more precipitous than the adsorption curve. This situation usually occurs when the distributions of pore size radii are wide. The presence of slit-shaped pores and/or panel-shaped particles generates the H3 and H4 curves. However, the exhibition of H4 loops indicates the existence of the micropore [36-41].

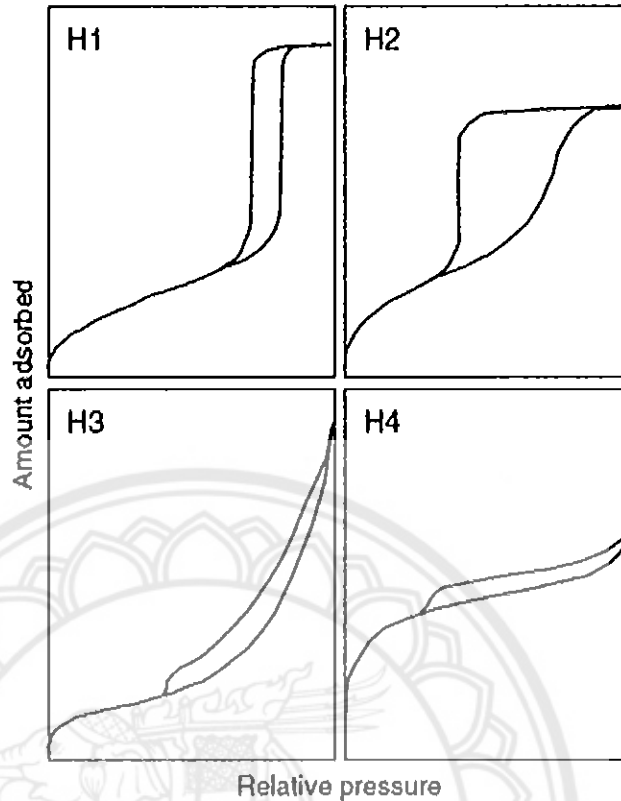


**Figure 2.1 The IUPAC classification of hysteresis loop.**

## 2.2 Variables affecting the adsorption isotherm

For a given pairs of adsorbate and adsorbent, the observable macroscopic variable; (a) the adsorbed amount versus chemical potential (or pressure), called the adsorption-desorption isotherm, and (b) the heat of adsorption versus loading, called the heat curve hereafter, are a complex function of a number of key variables:

- (1) Pore topologies: Simple pore, such as parallel slit, cylinder, sphere, to complex pores, such as arrays of varying sizes in the axial direction.
- (2) Surface affinity: Weak surface (such as silicon type) to strong surface (such as graphite)
- (3) Surface chemistry: Without functional group and with functional group: and type of functional groups (we restrict ourselves to dominant functional group commonly observed, such as phenolic, carbonyl and carboxylic) and their positions and orientation on the surface.
- (4) Adsorbate: Simple gases to associating fluids. Definitions of these adsorbates are given in the next section.

(5) Temperature: Sub-critical to supercritical. This is the most important variable as the mechanisms of adsorption and desorption, as well as the hysteresis and scanning curves, are strongly affected. It could be used as a useful variable to our advantage to tune the isotherm and the heat curve so that more information about the porous structure and surface chemistry could be derived.

### 2.3 Intermolecular Potentials

The model used to describe the intermolecular potential of the molecules in this work is the TraPPE-UA model [42-44] for CO<sub>2</sub> and CH<sub>4</sub>. For part of water we used TIP4P/2005 model [45]. The TraPPE-UA model and TIP4P/2005 model are used because they have been shown to describe the vapor-liquid equilibrium (VLE) really well and therefore should be the appropriate potential model to describe the adsorption systems [46, 47]. The parameters of each molecule are summarized in Table 2.1.

**Table 2.1 Potential parameters.**

Fluids	$x$ (nm)	$y$ (nm)	$z$ (nm)	$\sigma$ (nm)	$\epsilon/k_B$ (K)	$q$ (e)
<b>Water</b>						
O	0	0	0	0.31589	93.2	-
M	0	-0.01546	0	-	-	-1.1128
H(1)	-0.075695	-0.058588	0	-	-	+0.5564
H(2)	0.075695	-0.058588	0	-	-	+0.5564
<b>Carbon dioxide</b>						
O	0	0	0	0.3050	79	-0.35
C	0.116	0	0	0.2800	27	0.70
O	0.232	0	0	0.3050	79	-0.35
<b>Methane</b>						
CH <sub>4</sub> (1 site)	0	0	0	0.373	148	-



This work focused on the adsorption of  $\text{CO}_2$ ,  $\text{CH}_4$  and  $\text{H}_2\text{O}$  mixture. We show model of these fluids in Figure 2.2 and physical properties in Table 2.2.

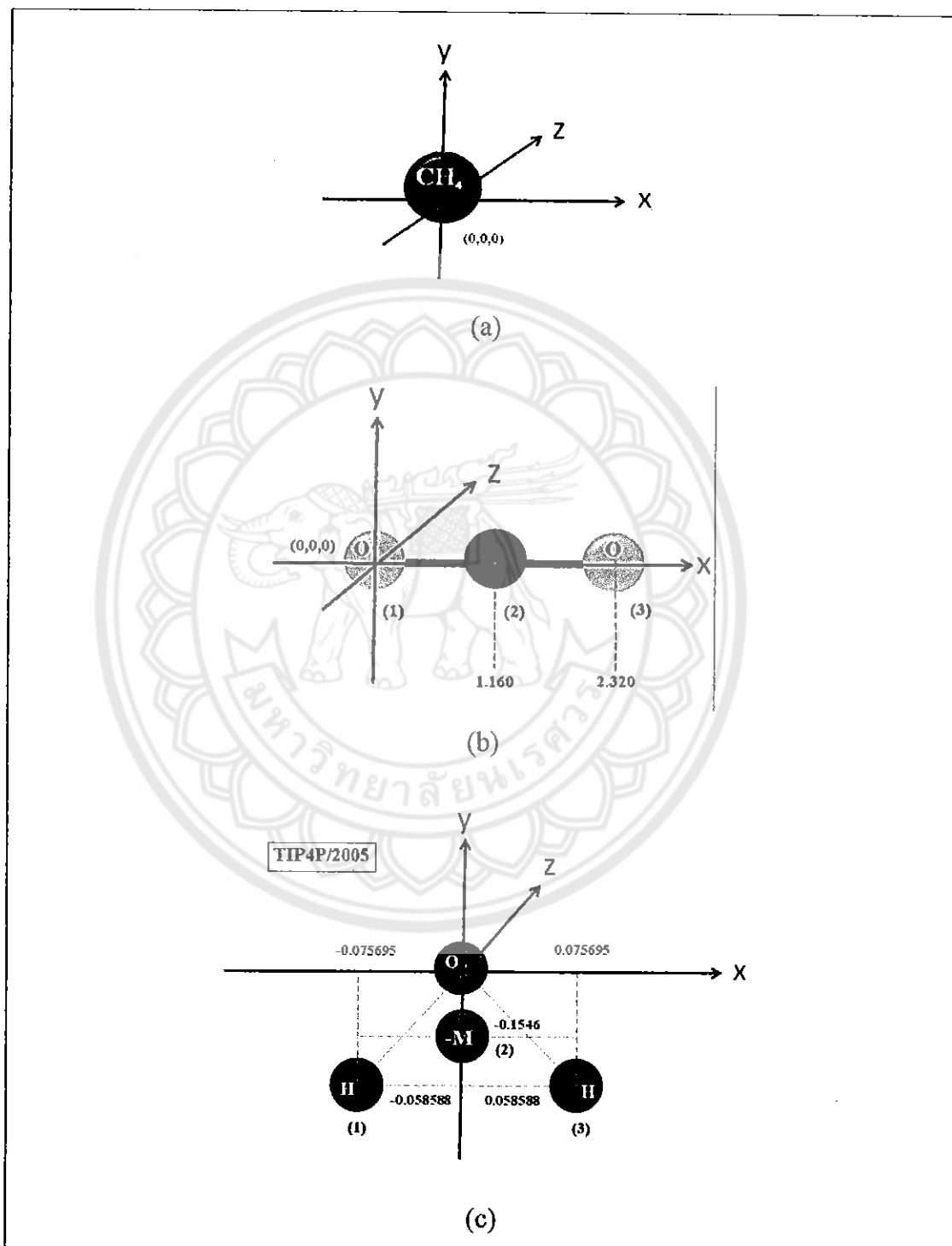


**Figure 2.2** The Models of fluid: (a) Methane; (b) Carbon dioxide and (c) Water TIP4P/2005.

**Table 2.2 Physical properties of Carbon dioxide, Methane and Water.**

Formula	Carbon dioxide CO <sub>2</sub>	Methane CH <sub>4</sub>	Water H <sub>2</sub> O
<b>Molecular weight</b>	44.0095	16.0425	18.0153
<b>Normal boiling point, T<sub>boil</sub>(K)</b>	216.6	111. ± 0.2	373.1243
<b>Critical temperature, T<sub>C</sub> (K)</b>	304.18	190.6 ± 0.3	647.096
<b>Critical pressure, P<sub>c</sub>(bar)</b>	73.80	46.1 ± 0.3	220.64
<b>Triple temperature, T<sub>triple</sub> (K)</b>	216.58	90.67 ± 0.03	273.16
<b>Triple pressure, P<sub>triple</sub> (bar)</b>	5.185	0.1169 ± 0.0006	0.0061
<b>Dipole moment (Debye)</b>	0.0	0.0	1.855

The non-bonded interactions of pseudoatoms are described by Lennard-Jones (LJ) interactions:

$$\varphi_{i,j}^{(a,b)} = 4\varepsilon^{(a,b)} \left[ \left( \frac{\sigma_{i,j}^{(a,b)}}{r_{i,j}^{(a,b)}} \right)^{12} - \left( \frac{\sigma_{i,j}^{(a,b)}}{r_{i,j}^{(a,b)}} \right)^6 \right] \quad (2.1)$$

where  $\varepsilon$  is the well depth of the interaction potential and  $\sigma$  is the collision diameter.  $i$  and  $j$  refer to particle  $i$  and particle  $j$ , while  $a$  and  $b$  refer to the LJ sites. The quadrupolar interactions of arene ring are described using three partial charges and the Coulomb potential:

$$\varphi_{i,j}^{(a,b)} = \frac{1}{4\pi\varepsilon_0} \cdot \frac{q_i^\alpha q_j^\alpha}{r_{i,j}^{(\alpha,\beta)}} \quad (2.2)$$

where  $\varepsilon_0$  is the permittivity of free space ( $\varepsilon_0 = 8.8543 \times 10^{-12} \text{ C}^2\text{J}^{-1}\text{m}^{-1}$ ).

The interaction potential between the adsorbate and the graphite surface is calculated with the Steele 10-4-3 equation [16]:

$$\varphi_{sf} = 4\pi\epsilon_{sf}\rho_s\sigma_{sf}^2 \left[ \frac{1}{5} \left( \frac{\sigma_{sf}}{z} \right)^{10} - \frac{1}{2} \left( \frac{\sigma_{sf}}{z} \right)^4 - \frac{\sigma_{sf}^4}{6\Delta(z+0.61\Delta)^3} \right] \quad (2.3)$$

where  $\rho_s$  is the surface density of solid,  $\Delta$  is the interlayer graphite spacing. The values of  $\rho_s$  and  $\Delta$  for graphite are  $38.2 \text{ nm}^{-2}$  and  $0.3354 \text{ nm}$ , respectively, while the molecular parameters  $\sigma_{ss}$  and  $\epsilon_{ss}/k_B$  for carbon are  $0.34 \text{ nm}$  and  $28 \text{ K}$ , respectively. The graphite slit-pore as shown in Figure 3 is considered in this work. The  $3 \text{ nm}$  pore width is considered as a mesoporous solid for the whole work.

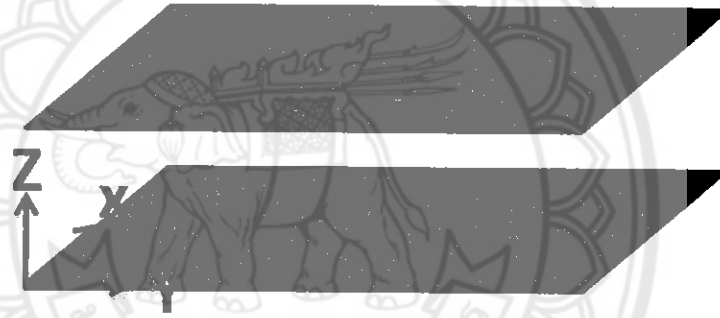


Figure 2.3 Graphitic slit-pore model.

The mixing rule used for determining the cross interaction parameters is the Lorentz-Berthelot (LB) mixing rules define as:

$$\sigma_{12} = \frac{1}{2}(\sigma_{11} + \sigma_{22}) \quad (2.4)$$

$$\epsilon_{12} = (\epsilon_{11} \cdot \epsilon_{22})^{1/2} \quad (2.5)$$

## 2.4 Methodology

Grand Canonical Monte Carlo (GCMC) Simulation is adsorption simulations are carried out using the grand canonical Monte Carlo technique [7, 8]. In GCMC, the temperature, volume and bulk pressure (chemical potential) are specified. For single component simulations, three types of trial are used: attempt to move and rotate, to delete, and to insert particles with microscopic reversibility requires such that an equal number of creation and deletion are made. In the multi-component simulations, the types of trial are similar to the pure component one but with an additional type of trial which is to swap the component identity of particles.

$$\text{Displacement: } P = \min \left\{ 1, \exp(-\beta(U_n - U_o)) \right\} \quad (2.6)$$

$$\text{Insertion: } P = \min \left\{ 1, \frac{z_i V}{N_i + 1} \exp[-\beta(U_n - U_o)] \right\} \quad (2.7)$$

$$\text{Deletion: } P = \min \left\{ 1, \frac{N_i}{z_i V} \exp[-\beta(U_n - U_o)] \right\} \quad (2.8)$$

$$\text{Swap } i \rightarrow j: P = \min \left\{ 1, \frac{z_j N_i}{z_i (N_j + 1)} \exp[-\beta(U_n - U_o)] \right\} \quad (2.9)$$

The subscripts  $i$  and  $j$  refer to the two components in a binary interaction,  $N$  is the number of molecules in the system before the MC move,  $V$  is the volume of the simulation box,  $\beta = 1/(k_B T)$  where  $k_B$  is the Boltzmann constant and  $T$  is the temperature,  $U_n$  and  $U_o$  are the energies of the configuration after and before the move, respectively, and  $z_i$  is the absolute activity given by,  $z_i = \exp(\mu_i/k_B T)/\Lambda^3$  where  $\Lambda$  is the thermal de Broglie wavelength.

The box length is more than 10 times the collision diameter for infinite length, and the cut-off radius taken to be half of the box length. The number of cycles for the equilibration and statistics collection steps was 50,000 each. In each cycle, there are 1,000 moves.

For the case of pore adsorption, the pore density ( $\rho_{\text{pore}}$ ) is defined in absolute and excess quantities

$$\rho_{\text{pore}}^{ABS} = \frac{\langle N \rangle}{V_{\text{acc}}}; \rho_{\text{pore}}^{EXC} = \frac{\langle N \rangle - \rho_b V_{\text{acc}}}{V_{\text{acc}}} \quad (2.10)$$

where  $\rho_b$  is the bulk molecular density,  $A$  is surface area of one wall of the simulation box,  $\langle N \rangle$  is the ensemble average of the number of particles in the pore, and  $V_{\text{acc}}$  is the accessible pore volume.

There are 4 Monte Carlo moves in Grand Canonical Monte Carlo (GCMC); (1) Insertion, (2) Deletion (3) Displacement Move and (4) Swap particles.

- (1) Insertion; A random position in the simulation box is selected to insert a particle. To accept the insertion the total energy of the system before and after move must be calculated. If the system is stable ( $U_{\text{total}} < 0$ ) we accept.
- (2) Deletion; A particle in the simulation box is selected randomly to delete. To accept the deletion the total energy of the system before and after move must be calculated. If the system is stable ( $U_{\text{total}} < 0$ ) we accept.
- (3) Displacement; A particle in the simulation box is selected randomly to displace. To accept the displacement move the total energy of the system before and after move must be calculated. If the system is stable ( $U_{\text{total}} < 0$ ) we accept.
- (4) Swap; A particle in the simulation box is selected randomly to be changed.

The number of cycles for an equilibration step and for statistics collection was 50,000. In each cycle, there are 1000 steps to insertion, deletion and displacement move with equal probability [31, 48, 49].

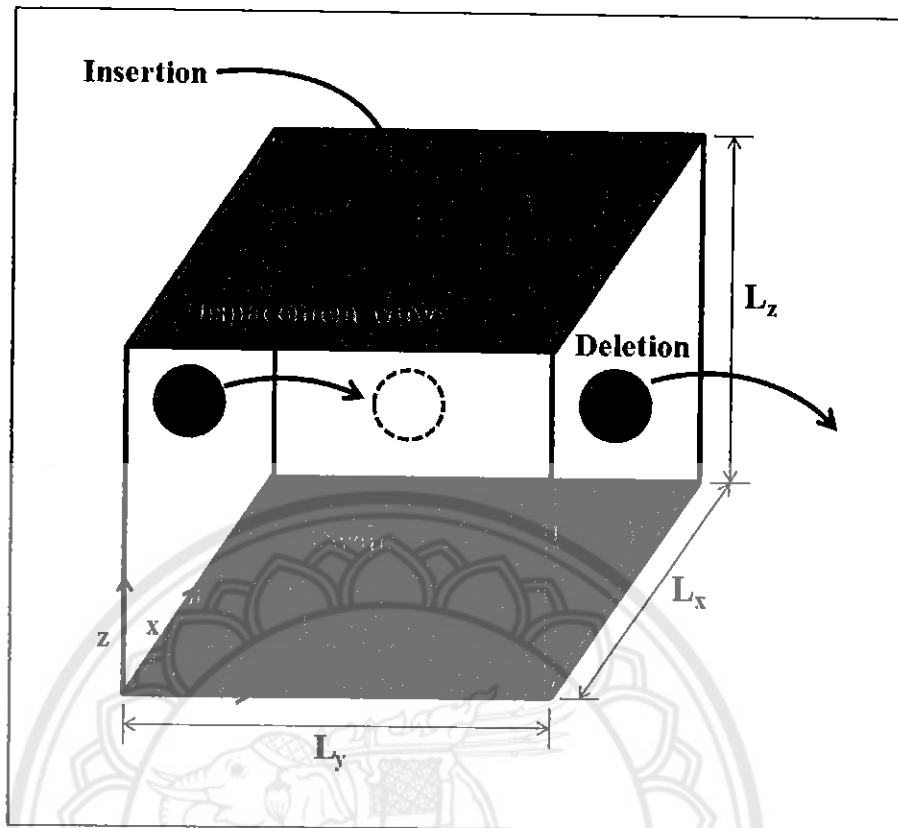


Figure 2.4 The grand canonical Monte Carlo (GCMC) simulation box.

Move proceeds as follows:

- (1) Randomly select the move type as an insertion or a deletion with equal probabilities; randomly select a particle  $j$  that acts as the target for the swap move.
- (2) If it is selected as an insertion move, then a particle chosen from the ideal gas phase is placed randomly inside the in region of particle  $j$ , or otherwise, if it is a deletion, then a particle to be deleted is chosen randomly from the in region of particle  $j$ .
- (3) Calculate the potential energy difference between the initial state.
- (4) Accept this move with the following set of acceptance probabilities.

## CHAPTER III

### RESULTS AND DISCUSSIONS

#### 3.1 Adsorption of CO<sub>2</sub>/CH<sub>4</sub> mixture

We first investigate the effects of temperature on the hysteresis loop of CO<sub>2</sub>/CH<sub>4</sub> mixture adsorption in 3nm width slit-pore as shown in Figure 3.1. As temperature is increased, we observe the following; (1) the hysteresis loop becomes smaller and disappeared at the critical hysteresis temperature because adsorption at high temperature has a high thermal motion that can be seen by the snapshots in Figure 3.1; (2) The selectivity of the mixture is slightly decrease with temperature increase which CO<sub>2</sub> dominates CH<sub>4</sub>. This point of view is advantaged for coal seam gas application that CH<sub>4</sub> can be replaced by CO<sub>2</sub>. The interesting is that we have known about pure component adsorption that when temperature is decrease the adsorbed amount is increased. This is true for the dominant CO<sub>2</sub> but opposite for the weaker CH<sub>4</sub>.

Interestingly, the hysteresis loop of the dominant CO<sub>2</sub> shows Type H1 which is a typical adsorption of a pure simple gas in slit-pore. In contrast, the hysteresis loop of CH<sub>4</sub> shows an abnormal type, the desorption branch at high pressures (where desorption branch of CO<sub>2</sub> leave its adsorption branch) is lower than its adsorption branch. Due to when the pore is just completed. The system is more packed for further pressure increase which the competition of CO<sub>2</sub> is extremely higher than CH<sub>4</sub>, resulting the decrease of CH<sub>4</sub> amount during the packing process. On the desorption, the pressure is decrease the mixture of packing in the pore is relaxed, get less structured adsorption. From this stage, CO<sub>2</sub> is initiated from a high packing than that of the previous lower pressure, while CH<sub>4</sub> is started from a lower packing than the previous lower pressures as mentioned above, The amount adsorbed of CH<sub>4</sub> is crossed the condensation branch then evaporated at the same pressure as CO<sub>2</sub> when pressure is further decreased. In the case for adsorption-desorption of CO<sub>2</sub>/CH<sub>4</sub> mixture (65:35) in 3 nm width slit-pore at 300 K and 180 K which according to the real composition in nature is provided in the Appendix which we found is tendency similar that of (1:1).

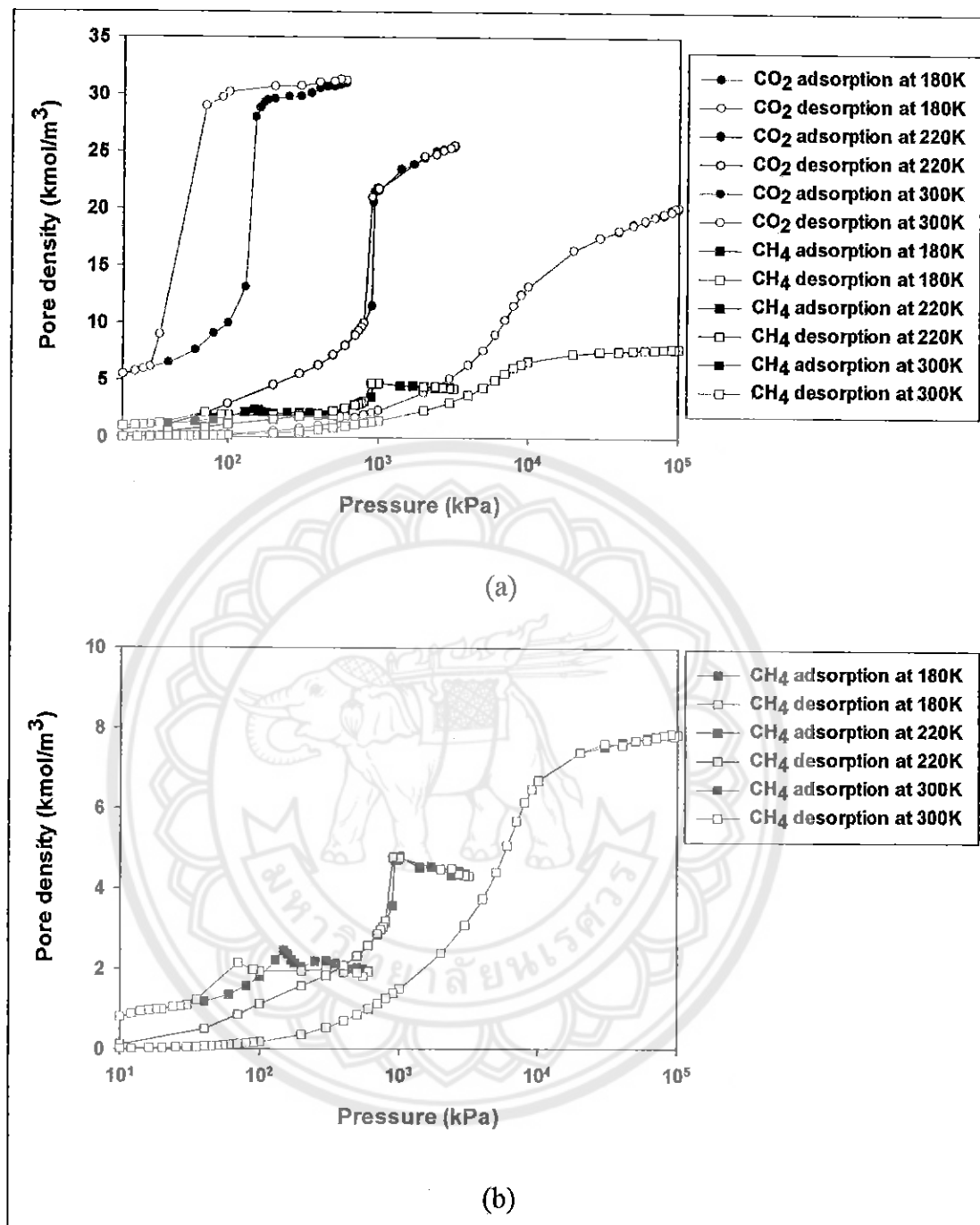
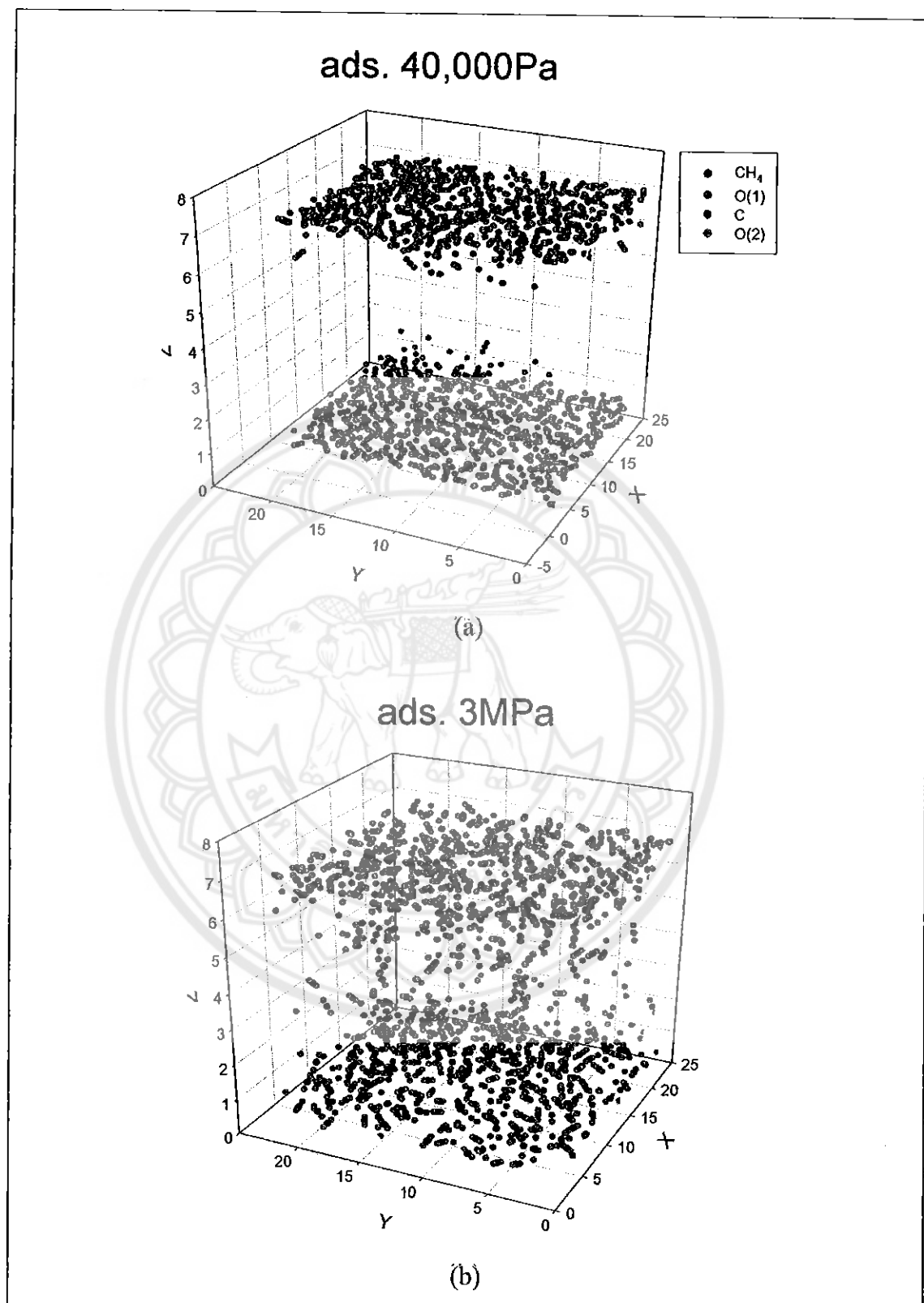


Figure 3.1 Adsorption-desorption of  $\text{CO}_2/\text{CH}_4$  mixture (1:1) in 3 nm width slit-pore at different temperature from 180-300 K: (a)  $\text{CO}_2$  and  $\text{CH}_4$  isotherms and (b)  $\text{CH}_4$  isotherms.

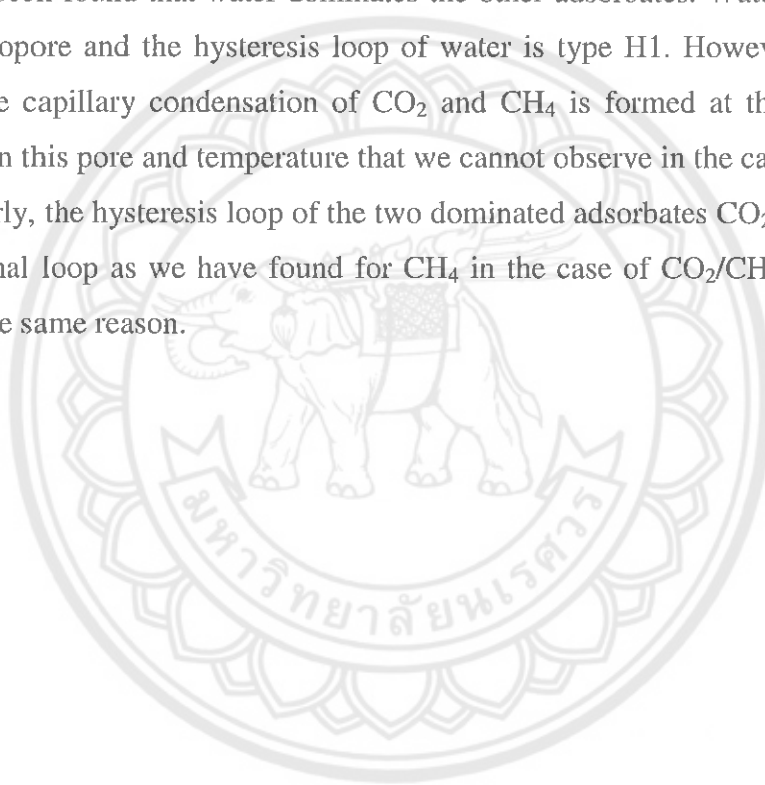




**Figure 3.2 Snapshots of CO<sub>2</sub>/CH<sub>4</sub> mixture (1:1) adsorption in the slit-pore at (a) 180 K and (b) 300 K, when monolayer is approximately completed.**

### 3.2 Adsorption of CO<sub>2</sub>/H<sub>2</sub>O and CH<sub>4</sub>/H<sub>2</sub>O mixtures

We then study the adsorption-desorption of CO<sub>2</sub> and CH<sub>4</sub> in the presence of water at 300 K. Because this conditions is operated in the real coal seam gas. The excess pore density of CO<sub>2</sub>/CH<sub>4</sub> as a function of pressure at 300 K is provided in the Appendix to compare with the excess pore density obtained from experimental work from the literature. The humidity is one of the problems in the real system. Water can affect the selectivity between CO<sub>2</sub> and CH<sub>4</sub> mixture. We present in Figures 3.3 and 3.4 CO<sub>2</sub>/H<sub>2</sub>O and CH<sub>4</sub>/H<sub>2</sub>O adsorptions, respectively, in 3 nm width slit-pore at 300 K. It has been found that water dominates the other adsorbates. Water can be condensed in mesopore and the hysteresis loop of water is type H1. However, very interesting that the capillary condensation of CO<sub>2</sub> and CH<sub>4</sub> is formed at the same pressure as water in this pore and temperature that we cannot observe in the case of without water. Similarly, the hysteresis loop of the two dominated adsorbates CO<sub>2</sub> and CH<sub>4</sub> shows the abnormal loop as we have found for CH<sub>4</sub> in the case of CO<sub>2</sub>/CH<sub>4</sub> in the last section with the same reason.



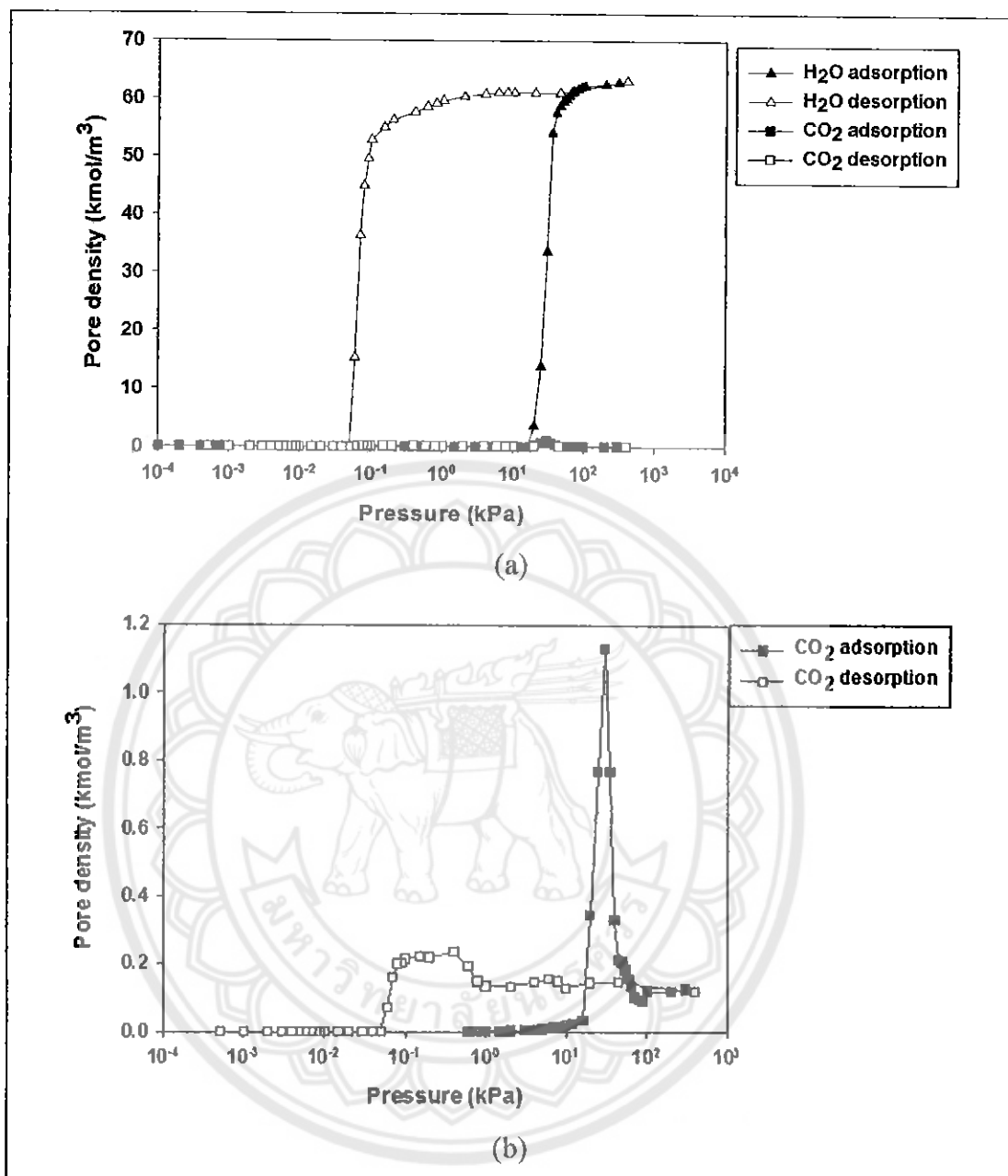


**Figure 3.3** Adsorption-desorption of CO<sub>2</sub>/H<sub>2</sub>O mixture (1:1) in 3 nm width slit-pore at 300 K: (a) CO<sub>2</sub> and H<sub>2</sub>O isotherms and (b) CO<sub>2</sub> isotherms.

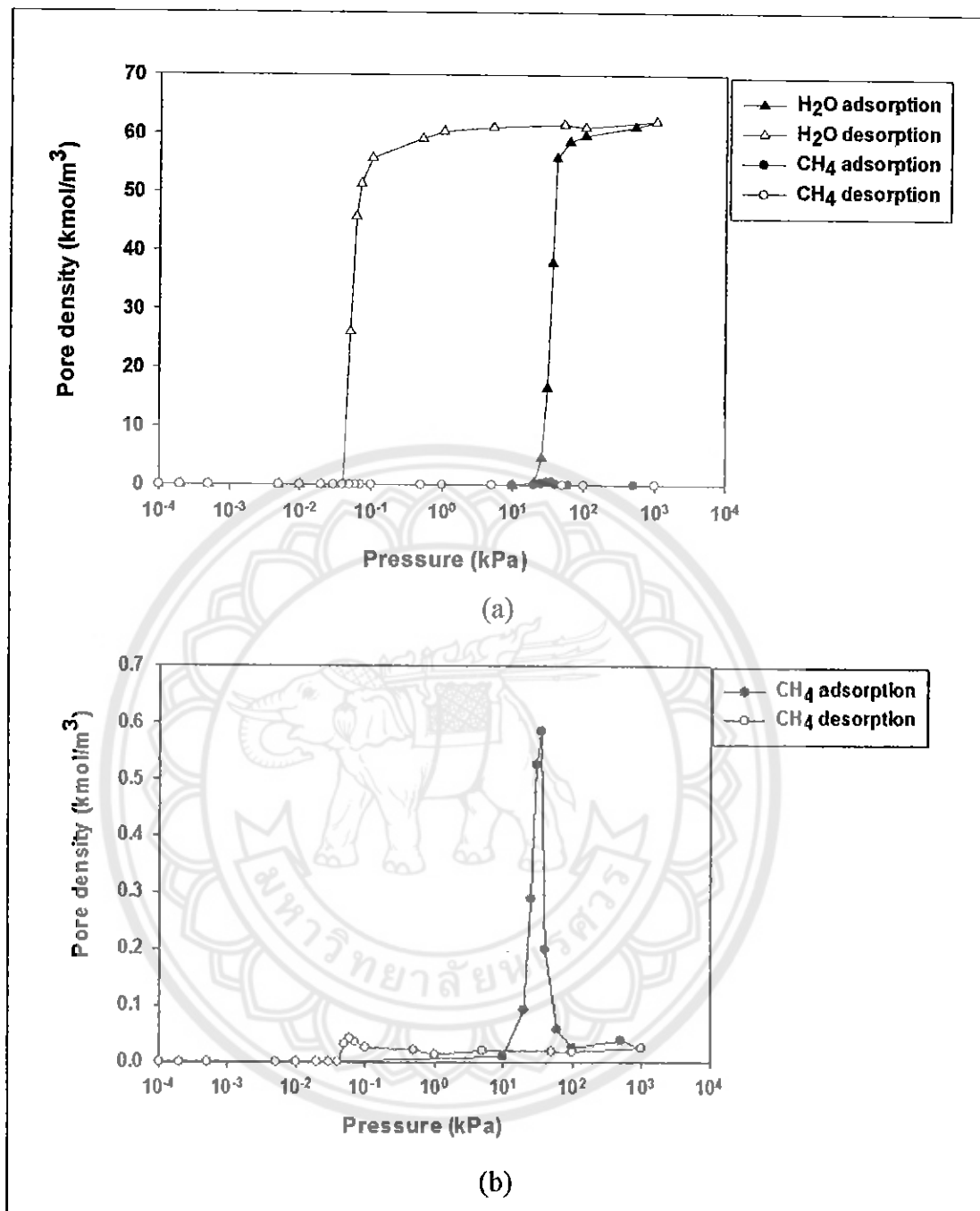


Figure 3.4 Adsorption-desorption of  $\text{CH}_4/\text{H}_2\text{O}$  mixture (1:1) in 3 nm width slit-pore at 300 K: (a)  $\text{CH}_4$  and  $\text{H}_2\text{O}$  isotherms and (b)  $\text{CH}_4$  isotherms.

### 3.3 Adsorption of CO<sub>2</sub>/CH<sub>4</sub>/H<sub>2</sub>O mixture

We now explain why the capillary condensation and evaporation of CO<sub>2</sub> and CH<sub>4</sub> can be found in this 3 nm width slit-pore at 300 K with in the presence of water. Figure 3.5 shows the adsorption-desorption of CO<sub>2</sub>/CH<sub>4</sub>/H<sub>2</sub>O mixture in 3 nm width slit-pores at 300 K. The hysteresis loop of water is Type H1. The condensation and evaporation of CO<sub>2</sub> and CH<sub>4</sub> are found at the same pressure of water.

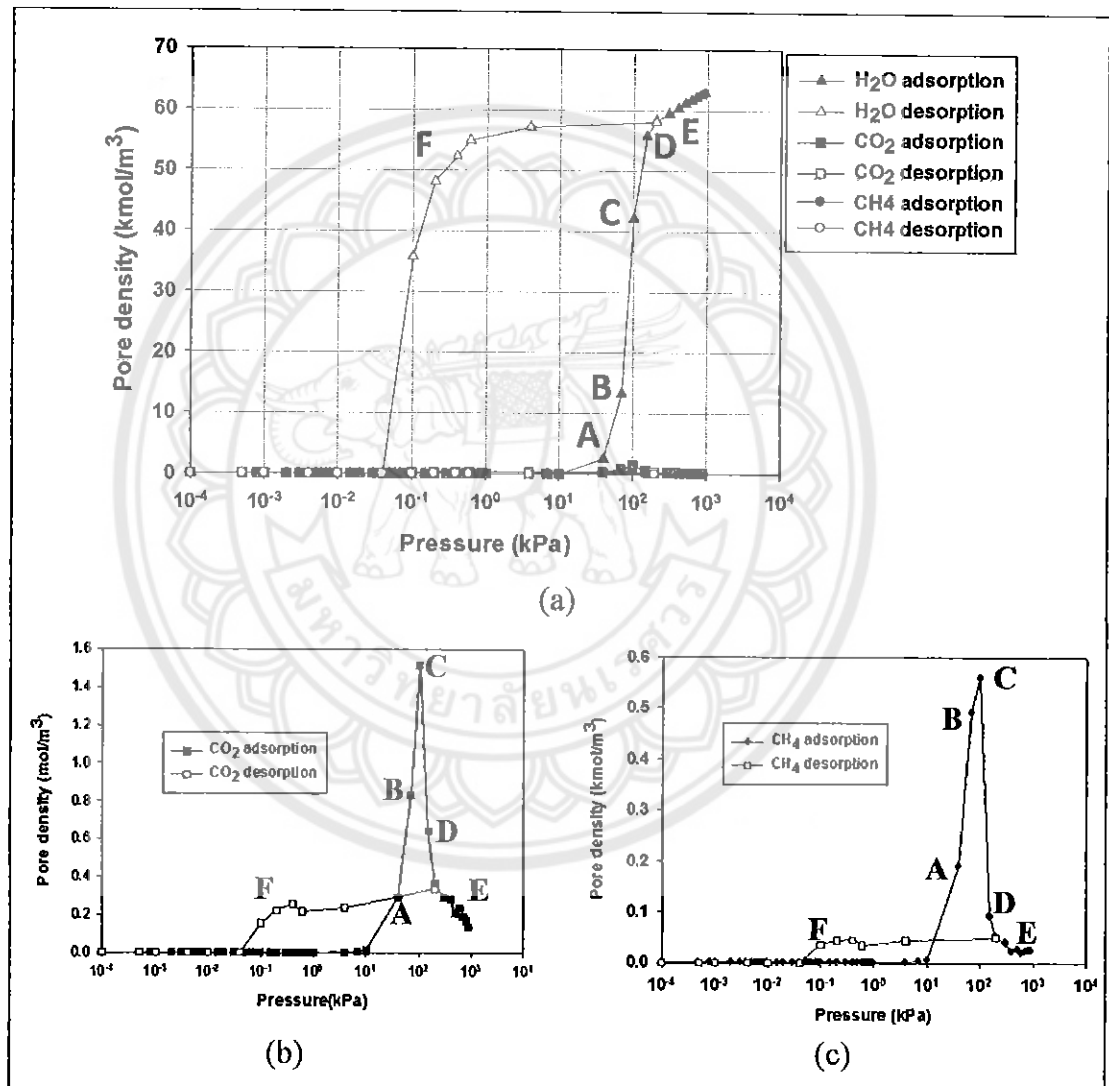
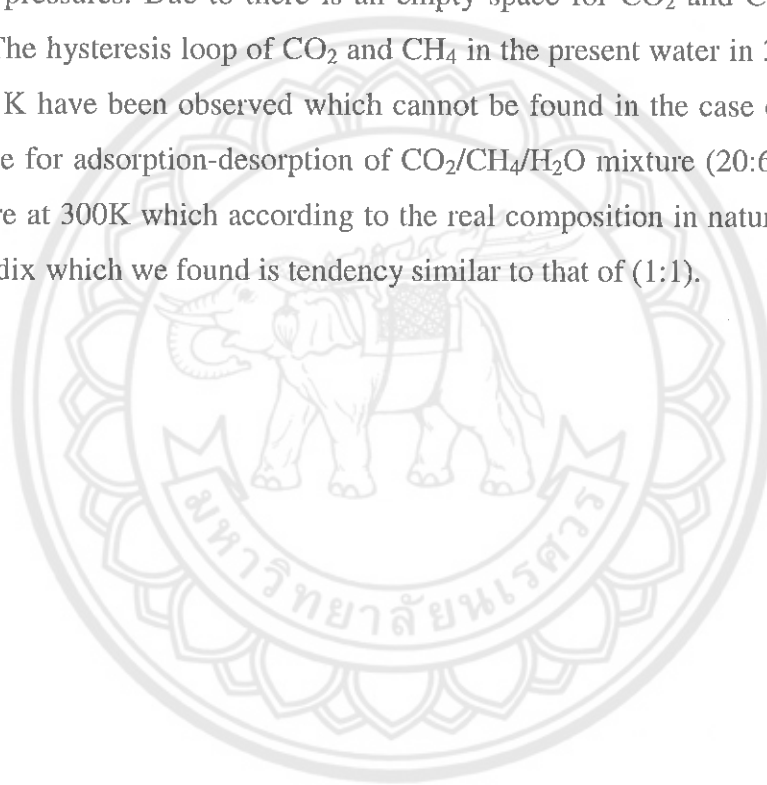
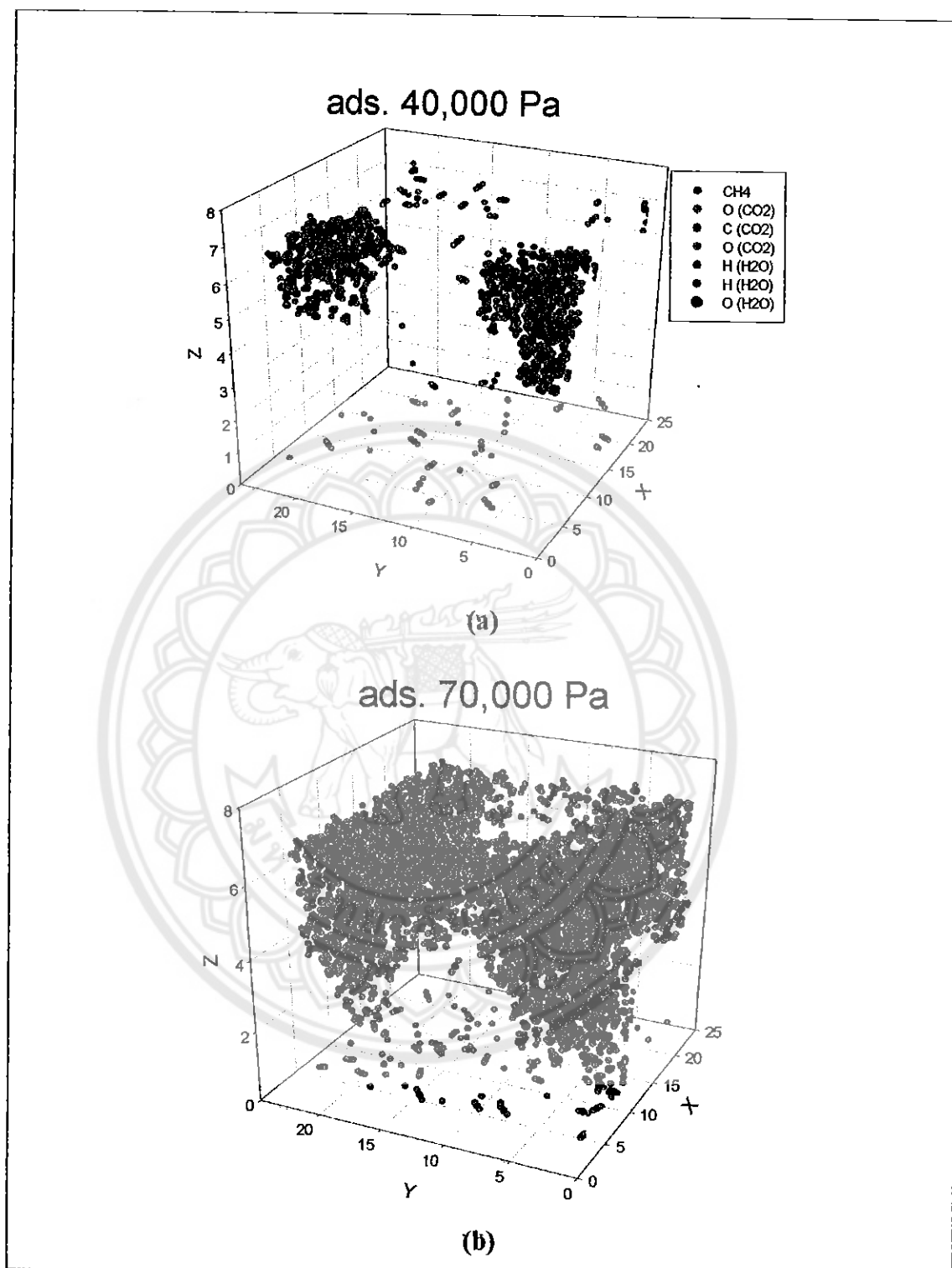


Figure 3.5 Adsorption-desorption of CO<sub>2</sub>/CH<sub>4</sub>/H<sub>2</sub>O mixture (1:1:1) in 3 nm width slit-pore at 300 K: (a) CO<sub>2</sub>, CH<sub>4</sub> and H<sub>2</sub>O isotherms; (b) CO<sub>2</sub> isotherms and (c) CH<sub>4</sub> isotherms.

When water cluster begins at the Point A,  $\text{CO}_2$  and  $\text{CH}_4$  are gradually increased, adsorbed into the empty space of pore as show by snapshots in Figure 3.6 Further pressure increases to Point B the sharp condensation of water is formed where water clusters merge together as shown by snapshot, resulting the empty space in the pore is smaller than  $\text{CO}_2$  and  $\text{CH}_4$  can be condensed. During the packing process at Points D and E, the amount adsorptions of  $\text{CO}_2$  and  $\text{CH}_4$  are extremely decrease as we have described in the last section. Upon the desorption, when water is gradually evaporated at Point F,  $\text{CO}_2$  and  $\text{CH}_4$  uptakes is slightly increased than the previous higher pressures. Due to there is an empty space for  $\text{CO}_2$  and  $\text{CH}_4$  to adsorb at this state. The hysteresis loop of  $\text{CO}_2$  and  $\text{CH}_4$  in the present water in 3 nm width slit-pore at 300 K have been observed which cannot be found in the case of without water. In the case for adsorption-desorption of  $\text{CO}_2/\text{CH}_4/\text{H}_2\text{O}$  mixture (20:65:15) in 3nm width slit-pore at 300K which according to the real composition in nature is provided in the Appendix which we found is tendency similar to that of (1:1).





**Figure 3.6** Snapshots of CO<sub>2</sub>/CH<sub>4</sub>/H<sub>2</sub>O mixture (1:1:1) in 3 nm width slit-pore at 300 K: (a) Adsorption at 40,000 Pa and (b) Adsorption at 70,000 Pa.

## CHAPTER IV

### CONCLUSIONS

We have presented condensation and evaporation of CO<sub>2</sub>, CH<sub>4</sub> and water mixtures in a mesoporous solid using GCMC. We have concluded by the following:

1. For adsorption of CO<sub>2</sub>/CH<sub>4</sub> mixture, the amount of CO<sub>2</sub> adsorbed is higher than that of CH<sub>4</sub>. This point of view is advantaged for coal seam gas application that CH<sub>4</sub> can be replaced by CO<sub>2</sub>.

2. For adsorption of CO<sub>2</sub>/CH<sub>4</sub>/H<sub>2</sub>O mixture. When water was introduced, the amount of CO<sub>2</sub> and CH<sub>4</sub> adsorbed is decreased. Water can be condensed more than that of CO<sub>2</sub> and CH<sub>4</sub>. Intermolecular forces of water are stronger than CO<sub>2</sub> and CH<sub>4</sub> to be the cause of a large hysteresis loop.

3. Temperature has an effect on adsorption. The height temperature, the amount of CO<sub>2</sub>/CH<sub>4</sub>/H<sub>2</sub>O mixture at 180 K adsorbed higher than at 300 K. The hysteresis loop becomes smaller and disappeared at the critical hysteresis temperature because adsorption at high temperature has a high thermal motion. So, the hysteresis loop at 180 K has a larger than at 300 K.

4. In the CO<sub>2</sub>/CH<sub>4</sub> mixture adsorption, the uptake of the dominant CO<sub>2</sub> is increased when temperature is decreased but it is opposite for the weaker CH<sub>4</sub>. The interesting is that we have known about pure component adsorption when temperature is decrease the adsorbed amount is increased. This is true for the dominant CO<sub>2</sub> but opposite for the weaker CH<sub>4</sub>.

5. The hysteresis loop of CO<sub>2</sub>/CH<sub>4</sub> mixture is disappeared at 300 K. However, when water is presented in the mixtures the hysteresis loop of CO<sub>2</sub> and CH<sub>4</sub> in the pore at 300 K is observed.





**REFERENCES**

## REFERENCES

1. Yang, R., Gas separation by adsorption processes Vol. 1. 1997, London, UK: Imperial College Press.
2. Doraiswamy, L.K., Catalytic reactions and reactors: A surface science approach. 1991, Oxford, UK: Pergamon Press.
3. Gregg, S.J. and K.S.W. Sing, Adsorption, surface area and porosity. 1982, London, UK: Academic Press.
4. Lee, A.K.K., Lattice theory correlation for binary gas adsorption equilibria on molecular sieves. Canadian Journal of Chemical Engineering, 1973. 51(6): p. 688-693.
5. Ross, S. and J.P. Olivier, On physical adsorption. 1964, New York, NY: Wiley-Interscience.
6. Myers, A.L. and J.M. Prausnitz, Thermodynamics of mixed-gas adsorption. AIChE Journal, 1965. 11(1): p. 121-127.
7. Allen, M.P. and D.J. Tildesley Computer simulation of liquids. 1989, Oxford: Oxford University Press. 385.
8. Frenkel, D. and B. Smit, Understanding molecular simulation: From algorithms to applications. 1996, San Diego: Academic Press. 443.
9. Ustinov, E.A. and D.D. Do, Modeling of adsorption in finite cylindrical pores by means of density functional theory. Adsorption, 2005. 11(5-6): p. 455-477.
10. El-Merraoui, M., M. Aoshima, and K. Kaneko, Micropore size distribution of activated carbon fiber using the density functional theory and other methods. Langmuir, 2000. 16(9): p. 4300-4304.
11. Cracknell, Roger F., David Nicholson, Stephen R. Tennison, Jill Bromhead, Adsorption and selectivity of carbon dioxide with methane and nitrogen in slit-shaped carbonaceous micropores: Simulation and experiment. Adsorption-Journal of the International Adsorption Society, 1996. 2(3): p. 193-203.
12. Tan, Z. and K.E. Gubbins, Selective adsorption of simple mixtures in slit pores - A model of methane ethane mixtures in carbon. Journal of Physical Chemistry, 1992. 96(2): p. 845-854.

13. Ravichandar Babarao, Sheng Dai, and De-en Jiang, Storage and separation of CO<sub>2</sub> and CH<sub>4</sub> in silicalite, C-168 schwarzite, and IRMOF-1: A comparative study from monte carlo simulation. *Langmuir*, 2007. 23(2): p. 659-666.
14. Qingyuan Yang, Chunyu Xue, Chongli Zhong and Jian-Feng Chen, Molecular simulation of separation of CO<sub>2</sub> from flue gases in Cu-BTC metal-organic framework. *AIChE Journal*, 2007. 53(11): p. 2832-2840.
15. Youn-Sang Bae, Karen L. Mulfort, Houston Frost, Patrick Ryan, Sudeep Punnathanam, Linda J. Broadbelt, Joseph T. Hupp and Randall Q. Snurr, Separation of CO<sub>2</sub> from CH<sub>4</sub> using mixed-ligand metal-organic frameworks. *Langmuir*, 2008. 24(16): p. 8592-8598.
16. Steele, W.A., The physical interaction of gases with crystalline solids: I. Gas-solid energies and properties of isolated adsorbed atoms. *Surface Science*, 1973. 36(1): p. 317-352.
17. Abdul Razak, M.a., D.D. Do, and G. Birkett, Evaluation of the interaction potentials for methane adsorption on graphite and in graphitic slit pores. *Adsorption*, 2011. 17(2): p. 385-394.
18. Klomkliang, N., D.D. Do, and D. Nicholson, Affinity and Packing of Benzene, Toluene, and p-Xylene Adsorption on a Graphitic Surface and in Pores. *Industrial & Engineering Chemistry Research*, 2012. 51(14): p. 5320-5329.
19. Klomkliang, N., D.D. Do, and D. Nicholson, On the hysteresis loop and equilibrium transition in slit-shaped ink-bottle pores. *Adsorption*, 2013: p. 1-18.
20. Klomkliang, N., D.D. Do, and D. Nicholson, On the hysteresis and equilibrium phase transition of argon and benzene adsorption in finite slit pores: Monte Carlo vs. Bin-Monte Carlo. *Chemical Engineering Science*, 2013. 87(0): p. 327-337.
21. Klomkliang, N., D.D. Do, and D. Nicholson, Effects of temperature, pore dimensions and adsorbate on the transition from pore blocking to cavitation in an ink-bottle pore. *Chemical Engineering Journal*, 2014. 239(0): p. 274-283.
22. Klomkliang, N., D.D. Do, and D. Nicholson, Hysteresis Loop and Scanning Curves of Argon Adsorption in Closed End Wedge Pores. *Langmuir*, 2014.

23. Nguyen, V.T., D.D. Do, and D. Nicholson, Microscopic configurations of methanol molecules in graphitic slit micropores: A computer simulation study. *J Colloid Interface Sci*, 2013. 396(0): p. 215-226.
24. Sizova, A.A., V.V. Sizov, and E.N. Brodskaya, Adsorption of CO<sub>2</sub>/CH<sub>4</sub> and CO<sub>2</sub>/N<sub>2</sub> mixtures in SBA-15 and CMK-5 in the presence of water: A computer simulation study. *Colloids and Surfaces A: Physicochemical and Engineering Aspects*, 2015. 474(0): p. 76-84.
25. Smykowski D, Nowak K, Łużny R, Szczygieł J, Szyja BM, The role of Ir<sub>4</sub> cluster in enhancing the adsorption of CO<sub>2</sub> on selected zeolites – GCMC simulations. *Journal of Molecular Graphics and Modelling*, 2015. 59(0): p. 72-80.
26. Junfang Zhanga, M.B. Clennella, D.N. Dewhursta, Keyu Liu, Combined Monte Carlo and molecular dynamics simulation of methane adsorption on dry and moist coal. *Fuel*, 2014. 122(0): p. 186-197.
27. Laurent Brochard, Matthieu Vandamme, Roland J.-M. Pellenq, and Teddy Fen-Chong, Adsorption-Induced Deformation of Microporous Materials: Coal Swelling Induced by CO<sub>2</sub>-CH<sub>4</sub> Competitive Adsorption. *Langmuir*, 2012. 28(5): p. 2659-2670.
28. Hyeon-Hui Leea, Hae-Jung Kima, Yao Shia, David Kefferb, Chang-Ha Lee, Competitive adsorption of CO<sub>2</sub>/CH<sub>4</sub> mixture on dry and wet coal from subcritical to supercritical conditions. *Chemical Engineering Journal*, 2013. 230(0): p. 93-101.
29. Hae Jung Kim, Yao Shi, Junwei He, Hyeon-Hui Lee, Chang-Ha Lee, Adsorption characteristics of CO<sub>2</sub> and CH<sub>4</sub> on dry and wet coal from subcritical to supercritical conditions. *Chemical Engineering Journal*, 2011. 171(1): p. 45-53.
30. Do, D.D. and H.D. Do, GCMC-surface area of carbonaceous materials with N<sub>2</sub> and Ar adsorption as an alternative to the classical BET method. *Carbon*, 2005. 43(10): p. 2112-2121.

31. Torrisi, A., R.G. Bell, and C. Mellot-Draznieks, Predicting the impact of functionalized ligands on CO<sub>2</sub> adsorption in MOFs: A combined DFT and Grand Canonical Monte Carlo study. *Microporous and Mesoporous Materials*, 2013. 168(0): p. 225-238.
32. Tongwei Zhanga, Geoffrey S. Ellisb, Stephen C. Ruppela, Kitty Millikena, Rongsheng Yanga, Effect of organic-matter type and thermal maturity on methane adsorption in shale-gas systems. *Organic Geochemistry*, 2012. 47(0): p. 120-131.
33. Keith Mosher, Jiajun He, Yangyang Liu, Erik Rupp, Jennifer Wilcox., Molecular simulation of methane adsorption in micro- and mesoporous carbons with applications to coal and gas shale systems. *International Journal of Coal Geology*, 2013. 109–110(0): p. 36-44.
34. Rahmati, M. and H. Modarress, Selectivity of new siliceous zeolites for separation of methane and carbon dioxide by Monte Carlo simulation. *Microporous and Mesoporous Materials*, 2013. 176(0): p. 168-177.
35. Puibasset, J. and R.J.M. Pellenq, A grand canonical Monte Carlo simulation study of water adsorption in a Vycor-like disordered mesoporous material at 300 K, in *Studies in Surface Science and Catalysis*, B.M.J.R. F. Rodriguez-Reinoso and K. Unger, Editors. 2002, Elsevier. p. 371-378.
36. Sylwester Furmaniak, Artur P. Terzyk, Piotr A Gauden, Peter J. F. Harris, Marek Wiśniewski, Piotr Kowalczyk., Argon adsorption in channel-like mesoporous carbons at 77 K: Grand Canonical Monte Carlo simulations and pore size analysis. *Microporous and Mesoporous Materials*, 2008. 116(1–3): p. 665-669.
37. Rahmati, M. and H. Modarress, Nitrogen adsorption on nanoporous zeolites studied by Grand Canonical Monte Carlo simulation. *Journal of Molecular Structure: THEOCHEM*, 2009. 901(1–3): p. 110-116.
38. A.Gotzias, H. Heiberg-Andersen, M. E. Kainourgiakis, Theodore A. Steriotis, Grand canonical Monte Carlo simulations of hydrogen adsorption in carbon cones. *Applied Surface Science*, 2010. 256(17): p. 5226-5231.

39. E. Pantatosakia, b, D. Psomadopoulosb, Th. Steriotisb, A.K. Stubosb, A. Papaioannoua, G.K. Papadopoulos, Micropore size distributions from CO<sub>2</sub> using grand canonical Monte Carlo at ambient temperatures: cylindrical versus slit pore geometries. *Colloids and Surfaces A: Physicochemical and Engineering Aspects*, 2004. 241(1–3): p. 127-135.
40. Horikawa, T., D.D. Do, and D. Nicholson, Capillary condensation of adsorbates in porous materials. *Adv Colloid Interface Sci*, 2011. 169(1): p. 40-58.
41. Klomkliang, N., D.D. Do, and D. Nicholson, On the hysteresis loop and equilibrium transition in slit-shaped ink-bottle pores. *Adsorption*, 2013. 19(6): p. 1273-1290.
42. Martin, M.G. and J.I. Siepmann, Transferable potentials for phase equilibria. I. United-atom description of n-alkanes. *The Journal of Physical Chemistry B*, 1998. 102(14): p. 2569-2577.
43. Wick, C.D., M.G. Martin, and J.I. Siepmann, Transferable potentials for phase equilibria. 4. United-atom description of linear and branched alkenes and alkylbenzenes. *Journal of Physical Chemistry B*, 2000. 104(33): p. 8008-8016.
44. Wick CD, Siepman JI, Klotz WL, Schure MR, Temperature effects on the retention of n-alkanes and arenes in helium-squalane gas-liquid chromatography - Experiment and molecular simulation. *Journal of Chromatography A*, 2002. 954(1-2): p. 181-190.
45. Abascal, J.L.F. and C. Vega, A general purpose model for the condensed phases of water: TIP4P/2005. *The Journal of Chemical Physics*, 2005. 123(23): p. 234505.
46. Do, D.D. and H.D. Do, Effects of potential models in the vapor–liquid equilibria and adsorption of simple gases on graphitized thermal carbon black *Fluid Phase Equilibria*, 2005. 236(1,2): p. 169-177
47. Do, D.D. and H.D. Do, Adsorption of argon on homogeneous graphitized thermal carbon black and heterogeneous carbon surface. *Journal of Colloid and Interface Science*, 2005. 287(2): p. 452-460.

48. Peng, X., D. Cao, and J. Zhao, Grand canonical Monte Carlo simulation of methane–carbon dioxide mixtures on ordered mesoporous carbon CMK-1. *Separation and Purification Technology*, 2009. 68(1): p. 50-60.
49. Chunyan Fana, D.D. Doa, D. Nicholsona, Jacek Jagiellob, Jeffrey Kenvinb, Marissa Puzanb, Monte Carlo simulation and experimental studies on the low temperature characterization of nitrogen adsorption on graphite. *Carbon*, 2013. 52(0): p. 158-170.

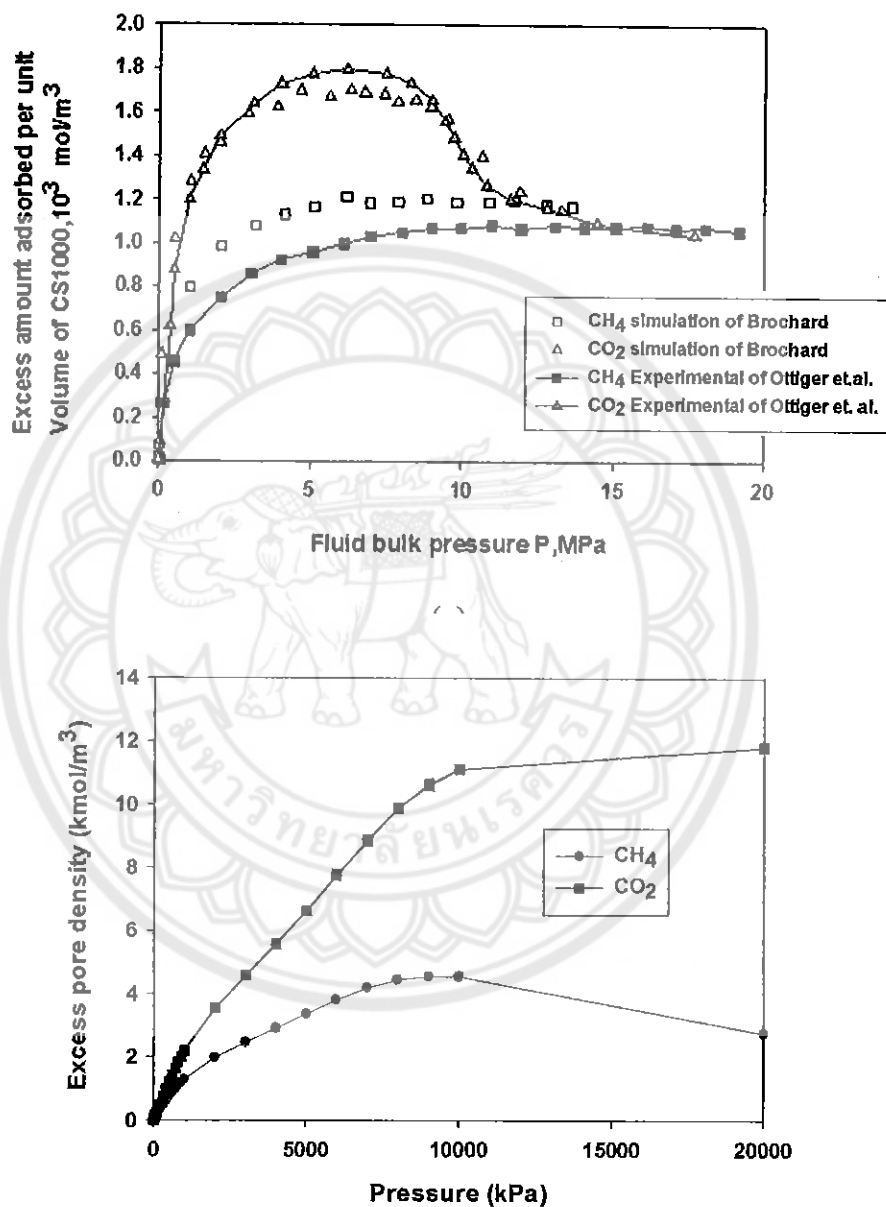






### Adsorption of CO<sub>2</sub>/CH<sub>4</sub> mixture

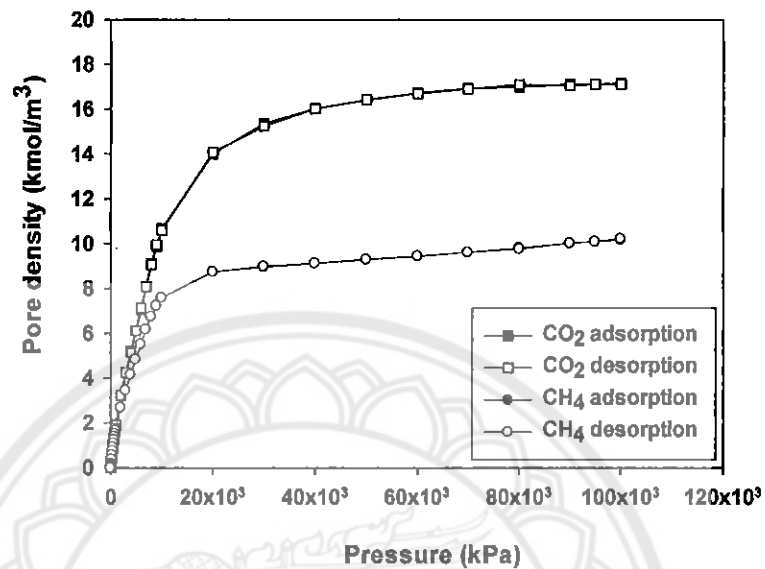
The excess pore density of CO<sub>2</sub>/CH<sub>4</sub> as a function of pressure at 300 K to compare with the excess pore density obtained from experimental work from the literature.



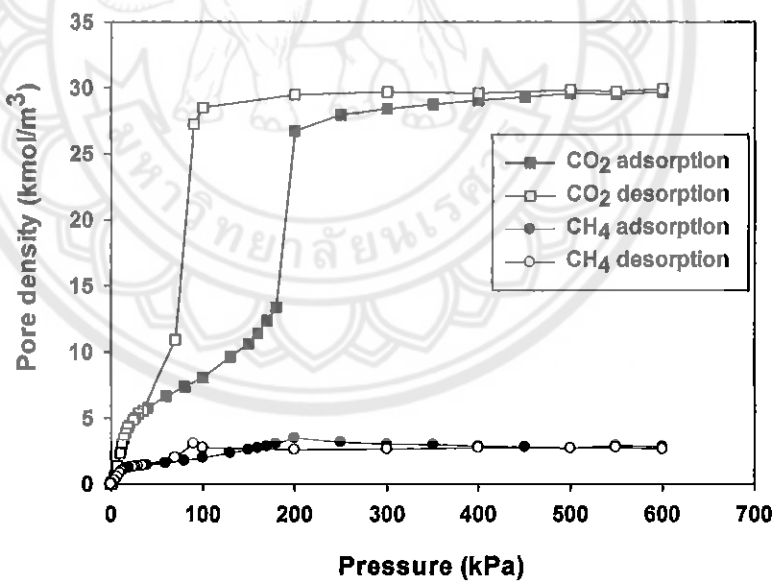
(b)

**Figure A1** The excess pore density of CO<sub>2</sub>/CH<sub>4</sub> as a function of pressure (a) The experimental data at 318.15 K are from the literature [27] (b) The results obtained from GCMC are at 300 K.

Adsorption-desorption of CO<sub>2</sub>/CH<sub>4</sub> mixture (35:65) in 3 nm width slit-pore at 300 K and 180 K which according to the real composition in nature (Figure A2)



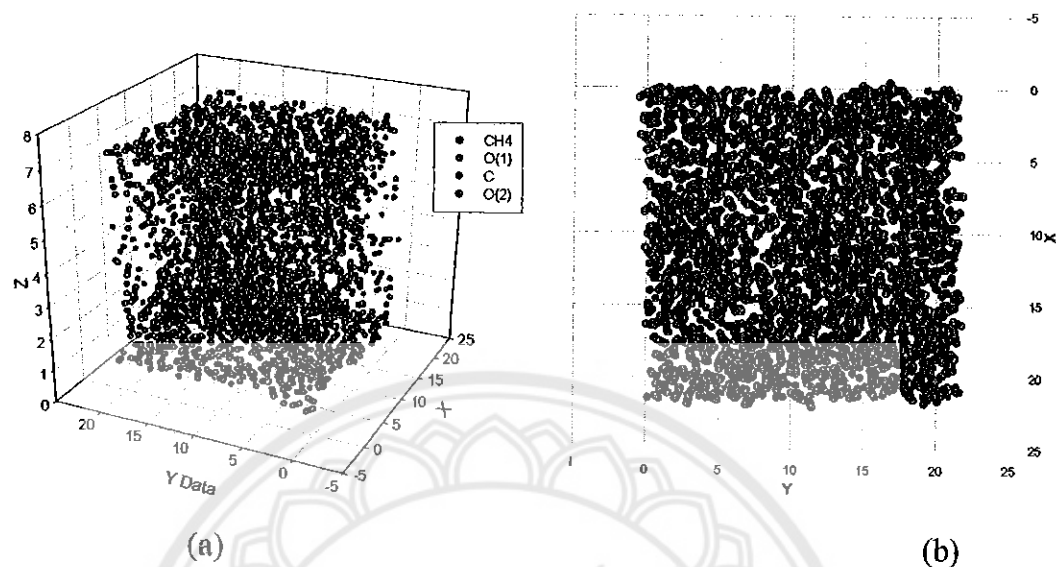
(a)



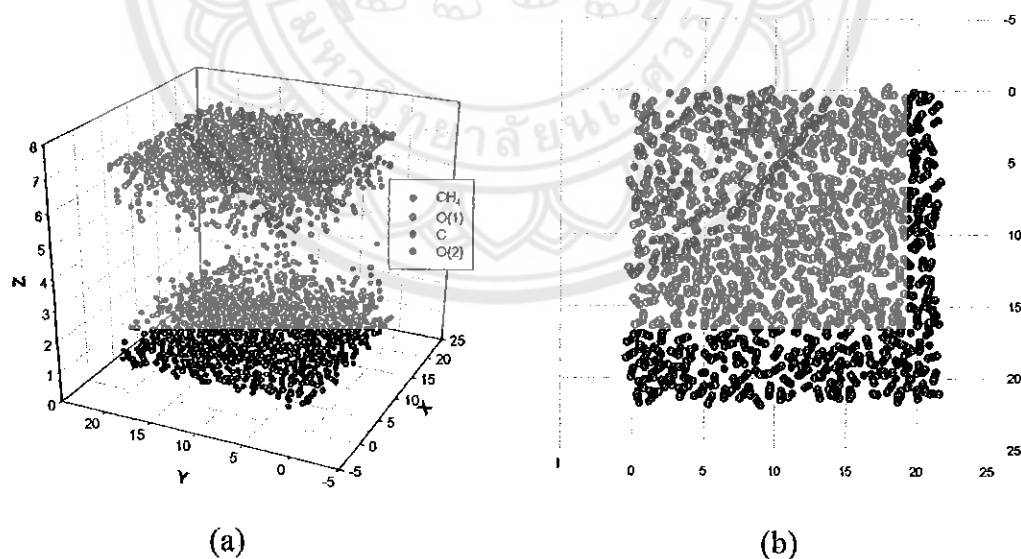
(b)

Figure A2 Adsorption-desorption of CO<sub>2</sub>/CH<sub>4</sub> mixture (35:65) in 3 nm width slit-pore: (a) at 300 K and (b) at 180 K.

To understand the microscopic picture of mixture adsorption on the slit pore, we presented in Figure A3 and A4.



**Figure A3 Snapshots of  $\text{CO}_2/\text{CH}_4$  mixture (35:65) adsorption in the slit-pore at 300 K: (a) Side view and (b) Top view when monolayer is approximately complete.**



**Figure A4 Snapshots of  $\text{CO}_2/\text{CH}_4$  mixture (35:65) adsorption in the slit-pore at 180 K: (a) Side view and (b) Top view when monolayer is approximately completed.**

### Adsorption of CO<sub>2</sub>/CH<sub>4</sub>/H<sub>2</sub>O mixture

Adsorption-desorption of CO<sub>2</sub>/CH<sub>4</sub>/H<sub>2</sub>O mixture (20:65:15) in 3nm width slit-pore at 300 K which according to the real composition in nature (Figure A5).

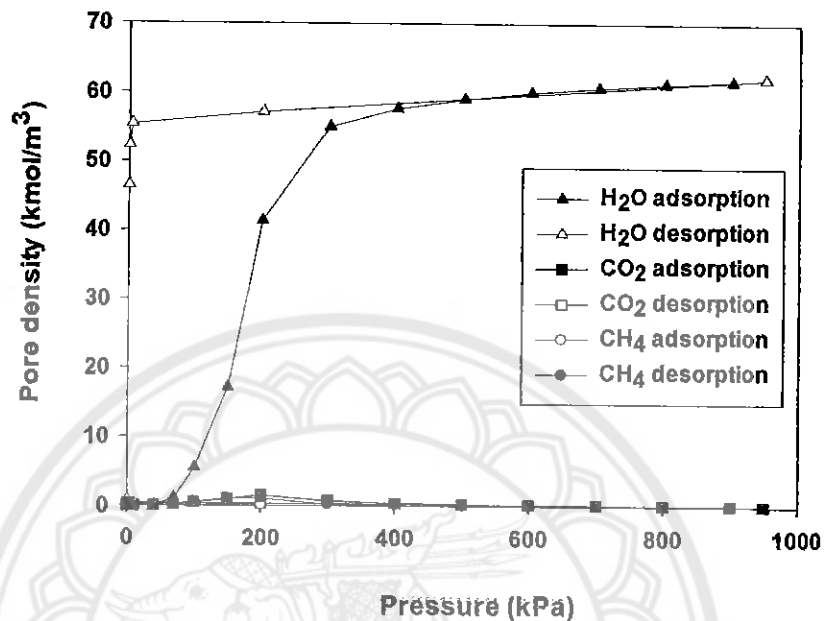


Figure A5 Adsorption-desorption of CO<sub>2</sub>/CH<sub>4</sub>/H<sub>2</sub>O mixture (20:65:15) in 3 nm width slit-pore at 300 K.

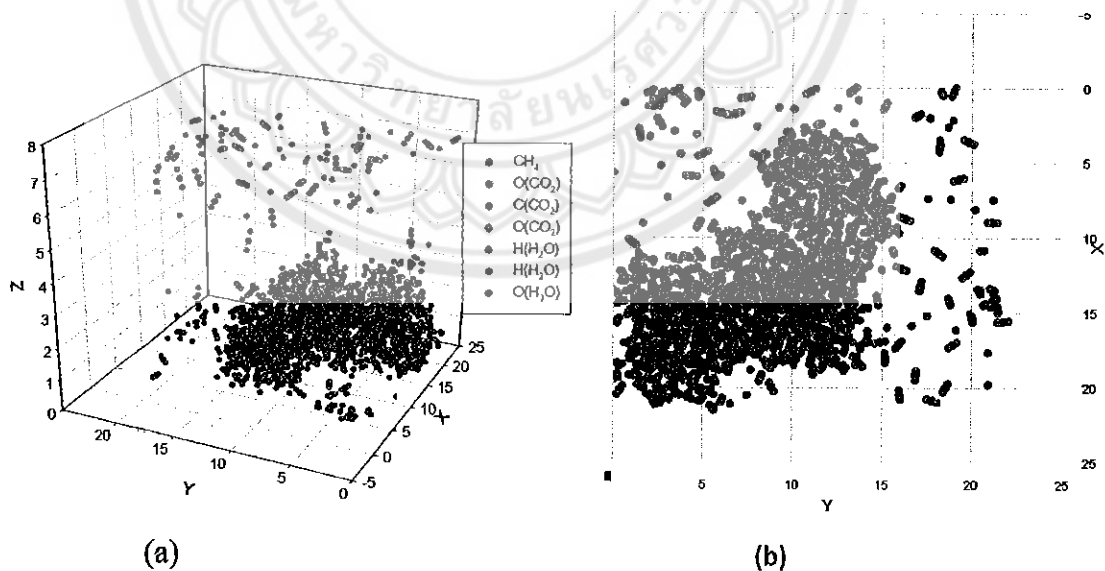


Figure A6 Snapshots of CO<sub>2</sub>/CH<sub>4</sub>/H<sub>2</sub>O mixture (20:65:15) adsorption in the slit-pore at 300 K: (a) Side view and (b) Top view.



## BIOGRAPHY

**Name –Surname** Natnaree Soitaku  
**Date of Birth** November 8, 1992  
**Place of Birth** Tak, Thailand  
**Address** 115/5, Maesod a, Amphor Maesod, Tak,  
Thailand. 63110

### Education Background

2014 B. Eng. (Chemical Engineering),  
Naresuan University, Thailand

**Name –Surname** Sutasinee Sooksai  
**Date of Birth** September 7, 1992  
**Place of Birth** Ubonratchatani, Thailand  
**Address** 352/8, Sansuk, Amphor Warinchamrab, Ubonratchatani,  
Thailand. 34190

### Education Background

2014 B. Eng. (Chemical Engineering),  
Naresuan University, Thailand